VOLUME 34 NUMBER 10

ACCOUNTS of CHEMICAL RESEARCH®

OCTOBER 2001

Supramolecular Arrays Based on Dimetal Building Units

F. ALBERT COTTON,*,† CHUN LIN,*,† AND CARLOS A. MURILLO*,†,‡

Department of Chemistry and Laboratory for Molecular Structure and Bonding, P.O. Box 30012, Texas A&M University, College Station, Texas 77842-3012, and Department of Chemistry, University of Costa Rica, Ciudad Universitaria, Costa Rica

Received March 27, 2001

ABSTRACT

Supramolecular chemistry is today a major thrust area, a significant part of which is based on the use of metal atoms or ions as key elements in promoting the assembly of and dictating the main structural features of the supramolecular products. Most of the work has been done with single metal atoms or ions in this role, but considerable success has already been achieved by employing M−M bonded dimetal entities instead. We review here the work done in our laboratory. Metal−metal bonded cationic complexes of the $[M_2(DAniF)_n(MeCN)_{8-2n}]^{(4-n)+}$ type, where M = Mo or Rh and DAniF is an *N*,*N*′-di-*p*-anisylformamidinate anion, have been used as subunit precursors and then linked by various equatorial and axial bridging groups such as polycarboxylate anions, polypyridyls, and polynitriles. Characterization of the products by single-crystal X-ray diffraction, CV, DPV, NMR, and other spectroscopic techniques has revealed the presence of discrete tetranuclear (pairs or loops), hexanuclear (triangles), octanuclear (squares), and dodecanuclear (cages) species and one-, two-, or three-dimensional molecular nanotubes. These compounds display a rich electrochemical behavior which is affected by the nature of the linkers.

Introduction

The synthesis and structural characterization of large, discrete molecules in which coordinated metal ions arekey structure-determining units is, at present, an intensely active research area.[1] This type of research began with the use of mononuclear coordination centers (that is, single metal ions, especially Pd^{2+} and Pt^{2+}, but also Zn^{2+}, Cd^{2+}, and Ag^{+}) as the geometry-setting metallic components in the synthesized arrays.

Beginning in early 1998 in this laboratory, the use of *di*metal units (e.g., Mo_2^{4+} and Rh_2^{4+}) to build supramolecular arrays has been pioneered. Although this field is still in its infancy, its basic outlines have been established, and other chemists are beginning to contribute to it. It is therefore time to present our first progress report.

We have employed dimetal units for five major reasons: (1) Dimetal units can be used to create neutral rather than highly positive oligomers and networks, which can then be oxidized in a controlled way, with retention of structural integrity. (2) An enormous range of metals (i.e., V, Nb, Cr, Mo, W, Tc, Re, Ru, Os, Co, Rh, Ir, Pd, Pt, and Cu) are potentially available to form homologous structures. (3) A very large variety of organic ligands may be used to vary solubility, pore sizes, electrochemical

* To whom correspondence should be addressed. E-mail: cotton@tamu.edu, chunlin@us.ibm.com, murillo@tamu.edu. F.A.C. is Welch-Doherty Distinguished Professor, C.A.M. is adjunct Professor and Senior Lecturer (on leave from the University of Costa Rica), and C.L. is a Research Associate, all at Texas A&M University.

† Texas A&M University.

‡ University of Costa Rica.

F. Albert Cotton was born in Philadelphia, PA, in 1930 and received his A.B. and Ph.D. degrees from Temple and Harvard Universities, respectively. He was on the faculty of MIT from 1955 to 1971 and has been at Texas A&M since 1972. He has been recognized by both ACS awards in inorganic chemistry, the ACS Priestley Medal, the AIC Gold Medal, the Robert A. Welch Prize, the King Faisal Prize, the Paracelsus Prize, the Wolf Prize, the Lavoisier Medal, and the National Medal of Science. His interests have been in inorganic, organometallic, and structural chemistry. He discovered the existence of quadruple bonds, as well as related triple, double, and single bonds in a similar structural context, and has explored their chemistry extensively.

Chun Lin was born in Fuzhou, P. R. China, in 1969. He earned his B.S. degree in chemistry and materials science from the University of Science & Technology of China in 1992. He came to the United States in 1993. He obtained his Ph.D. from Florida Institute of Technology in inorganic chemistry in 1997 with Professor T. Ren. He then moved to Cotton's group as a research associate, where he pioneered the concept of introducing metal−metal bonds into supramolecular chemistry. He joined IBM, T. J. Watson Research Center, in June 2001. His research interests span aspects of materials chemistry, molecular-level devices and machines, nanoscience, inorganic synthetic chemistry, and metal-containing supramolecular chemistry. For more information visit www.chunlin.net.

Carlos A. Murillo was born in 1951 in Costa Rica. He received a bachelor's degree from the University of Costa Rica and a Ph.D. from Texas A&M University. After a postdoctoral stay at Princeton University, he returned to the University of Costa Rica, where he is a professor of chemistry and a charter member of the Costa Rican Academy of Sciences. He is also executive director of the Laboratory for Molecular Structure and Bonding, an adjunct professor, and a member of the graduate faculty at Texas A&M University.

10.1021/ar010062+ CCC: $20.00
Published on Web 08/17/2001

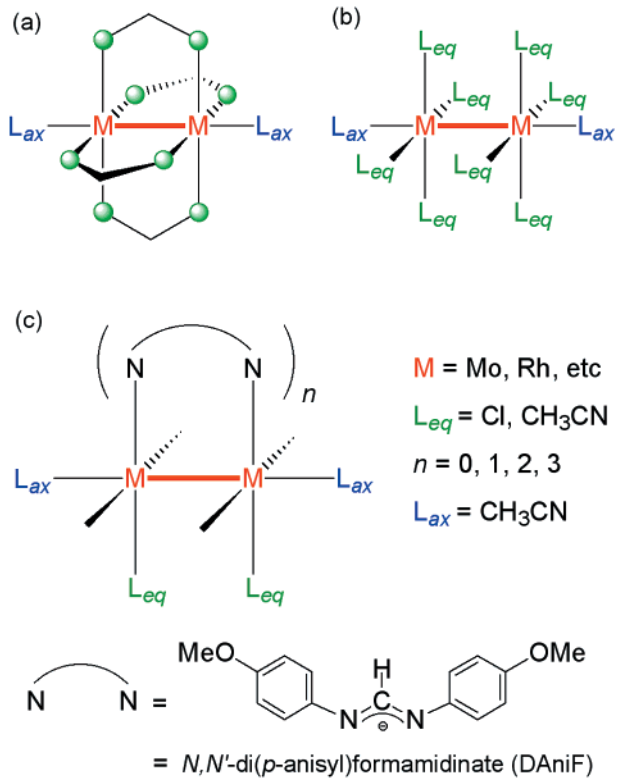

FIGURE 1. (a) A generic structure of a paddlewheel complex having four bridging groups and two axially coordinated ligands (which can be absent in some compounds). (b) A similar structure with eight equatorial monodentate ligands and two axially coordinated ligands. (c) Metal−metal bonded units used in the formation of extended structures.

activity, and other properties. (4) The spectroscopic and magnetic properties of dimetal units are extremely varied, and thus the arrays containing them can be designed with an extremely diversified range of such electronic properties. (5) By suitable choice of both equatorial and axial connecting elements, an enormous range of structures is available, and the nature and degree of interaction between adjacent dimetal units can be finely controlled.

During the past three decades, there has been remarkable progress in the understanding of dinuclear compounds containing multiple metal−metal bonds.[2] The paddlewheel structural motif (Figure 1a) commonly adopted by this class of complexes has three important features: (1) Transition metal atoms of groups 5−10 can come together to form M−M bonds with formal bond orders varying from four to zero. (2) The equatorial ligands (green) can be bridging, e.g., carboxylates, formamidinates, or monodentate such as halide ions. Each metal atom is in a square-planar or pyramidal configuration with regard to four such equatorially coordinated atoms. (3) Some metals, such as Cr, Rh, Ru, and Re, have a strong preference for axial coordination. The axial ligands (blue) frequently contain N- or O-donating atoms.

For this class of compounds, both the experimental and the theoretical aspects of the chemistry have been explored extensively, providing a tremendous amount of information in several areas: the reactivities of compounds; the strengths of metal−metal interactions; the electronic transitions between metal-based orbitals, as well as those involving metal-to-ligand charge transfers; the redox activities of the dinuclear cores; and the correlation among these properties. Nevertheless, much is still to be learned about the fundamentals of the chemistry of compounds containing metal−metal bonds.

Strategy and Assembly Schemes

Making a supramolecule is somewhat like constructing a building, which starts with bricks as subunits, and cement as a linker. These two components are put together first to form a wall, but eventually into an entire building. Based on a similar strategy, *di*metal units, with the well-known paddlewheel framework shown on the left of Figure 1a, are employed as the subunits, and various ligands, usually organic but not necessarily, are the linkers. These two components self-assemble into the target supramolecules as long as they have matching dimensions and shapes, as in Stang's "molecular library" scheme.[1b]

The correct choices of subunits and linkers are critical for success. The dimetal subunits that we commonly use are sketched in Figure 1c. These precursors have been carefully designed so that some edges of the paddlewheel are rendered relatively unreactive by a nonlabile formamidinate bridge, while the remaining coordination sites are occupied by easily displaceable ligands, such as acetonitrile or chloride ions. The formamidinate bridges can be made with many different substituent groups. We have found that the *p*-anisyl group (i.e., *N*,*N*′-di-*p*-anisylformamidinate, abbreviated as DAniF) provides good solubility properties. Our equatorial linkers are usually polycarboxylic acid anions, which have generally been used in the form of their organic-soluble R_4N^+ salts. The axial linkers can be various kinds of polynitriles and polypyridyls containing N-donor atoms. Just a few of a huge number of possibilities for linkers are given in Figure 2.

Based on our choices of subunits and linkers, three basic assembly schemes can be established (Figure 3). Two metal−metal bonded units can be joined together face-to-face with an equatorial linker, end-to-end with an axial linker, or in larger assemblies by a combination of these modes of linkage. These assembly schemes are capable of producing as great a variety of structures as are the single-metal moieties but with the five advantages mentioned earlier. It should be pointed out that the key to this work has been the precise control we have developed for the preparation of the starting materials, whereby stepwise substitution of the formamidinates can accomplished to give, for example, compounds of the type $[Mo_2(DAniF)_n(CH_3CN)_{2(4-n)}]^{(4-n)+}$ where *n* can vary from 0 to 4.[3]

Pairs of $M_2(DAniF)_3$ Units

Our first achievement was to bring together sets of two M_2 units to form "dimers of dimers", or pairs as we have

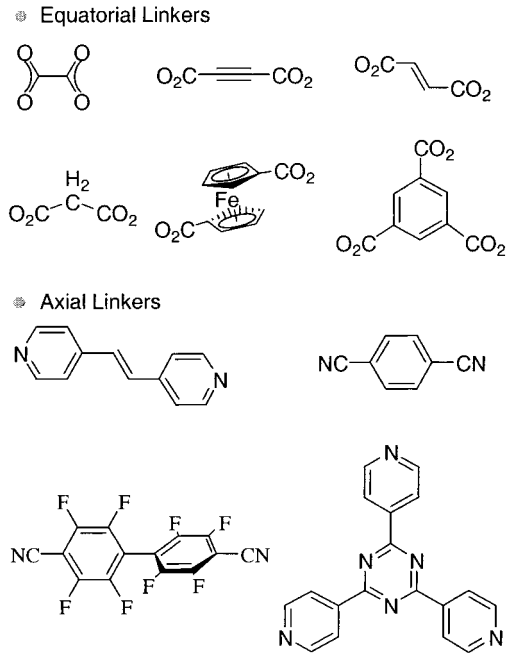

FIGURE 2. A few of the polycarboxylato polyanions used as linkers with a selection of neutral nitrogen-containing molecules employed as axial linkers.

called them.[4,5] This is best accomplished by the following one-pot reaction:

$$2Mo_2(DAniF)_3(CH_3CN)_2(BF_4) + (NEt_4)_2(O_2C{-}\square{-}CO_2) \xrightarrow{CH_3CN} (DAniF)_3Mo_2(O_2C{-}\square{-}CO_2)Mo_2(DAniF)_3 + 2NEt_4BF_4$$

Twelve compounds containing two quadruply bonded $Mo_2(DAniF)_3$ units linked by various dicarboxylate anions have been prepared in high purity and good yields. As described by the linkers, the compounds are oxalate, **1**; acetylene dicarboxylate, **2**; fumarate, **3**; tetrafluoroterephthalate, **4**; carborane dicarboxylate, **5**; ferrocene dicarboxylate, **6**; malonate, **7**; succinate, **8**; propane-1,3-dicarboxylate, **9**; tetrafluorosuccinate, **10**; bicyclo[1.1.1]-pentane-1,3-dicarboxylate, **11**; and *trans*-1,4-cyclohexanedicarboxylate, **12**. This general synthetic methodology can be applied to link any $M_2(DAniF)_3$ unit with virtually any dicarboxylic acid, as long as its tetraalkylammonium salt and the necessary dimetal precursor can be prepared. Single-crystal X-ray work has been carried out for all 12 compounds. A typical molecular structure is shown in Figure 4 for the oxalate derivative. Generally, the two Mo—O—□—O—Mo planes are either coplanar or form a step, depending on the geometry of the dicarboxylate linkers, with the Mo—Mo axes nearly parallel to each other.

A feature of these compounds to which we have devoted considerable attention is their electrochemistry. The degree of electronic coupling of two Mo_2 centers through the linkers can be gauged by the separation of their half-wave potentials ($E_{1/2}$), and the results can be rationalized with the help of Scheme 1. After the first one-electron oxidation of the compound, for which the half-wave potential is $E_{1/2}$(I), there are two extreme cases. In

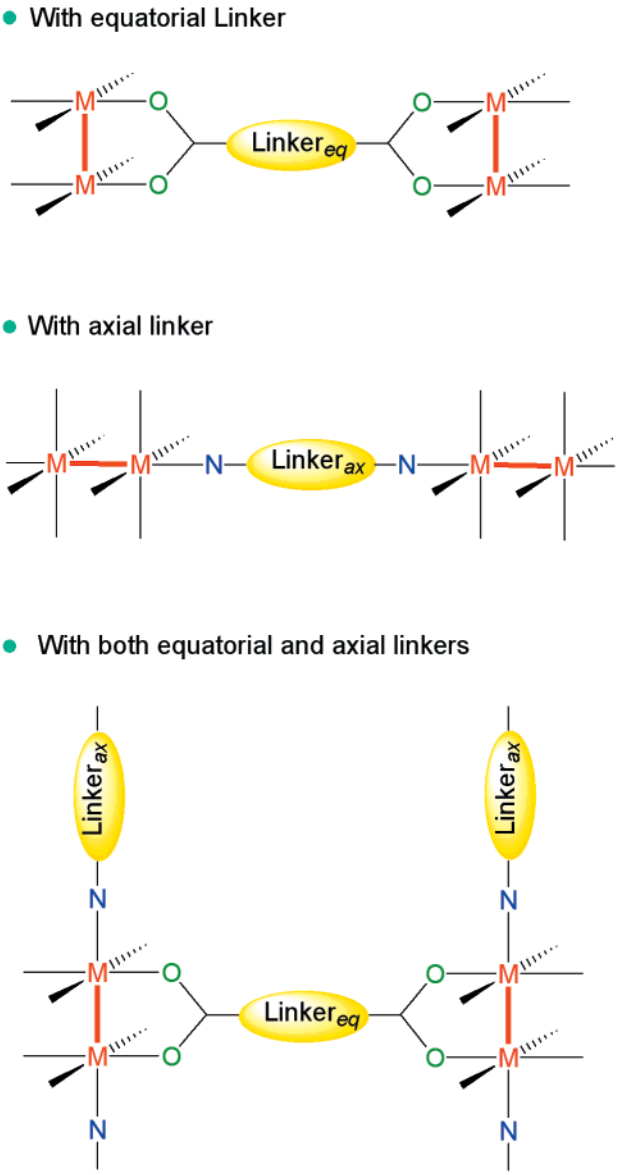

FIGURE 3. Schemes of three basic modes of assembly of dinuclear units.

one, the positive charge is *localized*, that is, carried entirely by one of the two Mo_2 centers, and there is only a remote effect on the second Mo_2 center. In the other case, the charge is *delocalized*, that is, the positive charge is evenly distributed over the two Mo_2 units, and each Mo_2 unit carries approximately a half-positive charge. In the former case, the second one-electron oxidation is on an uncharged Mo_2 center, and therefore $E_{1/2}$(II) should be very close to $E_{1/2}$(I). In the latter case, the second one-electron oxidation is on a half-positively charged Mo_2 center, and $E_{1/2}$(II) should obviously be much more positive than $E_{1/2}$(I). Cyclic voltammograms (CV) and differential pulse voltammograms (DPV) of the 12 compounds provided the data shown in Figure 5.

For all but three compounds, these data are as expected for no delocalization, that is, the value of $\Delta E_{1/2}$ is determined by electrostatics. For the three points above the line, it is believed that some degree of charge delocaliza-

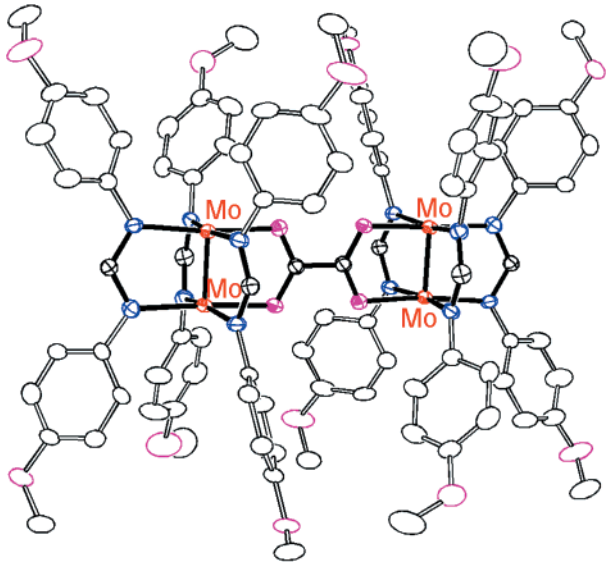

FIGURE 4. The molecular structure of pair **1** having two essentially parallel quadruply bonded Mo_2 units linked by an oxalate anion. For this and all other drawings having thermal ellipsoids, the color code is red for the metal atoms, blue for the nitrogen atoms, and purple for the oxygen atoms.

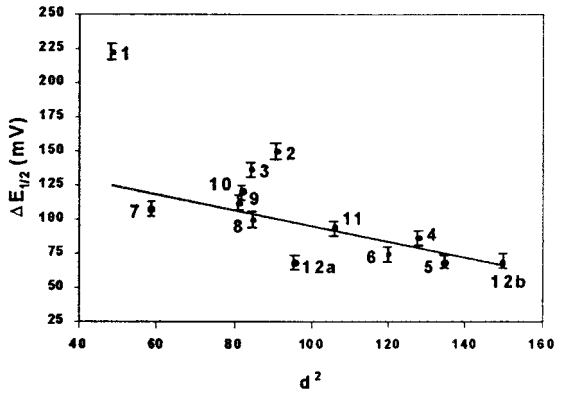

FIGURE 5. Variation of the separation of the electrochemical potentials for the oxidation of each of the two Mo_2 units for the pairs **1**−**12** as a function of the square of the distance between the midpoints of the Mo−Mo bonds. Pairs **1**−**3** show greater delocalization than **4**−**12**.

Scheme 1

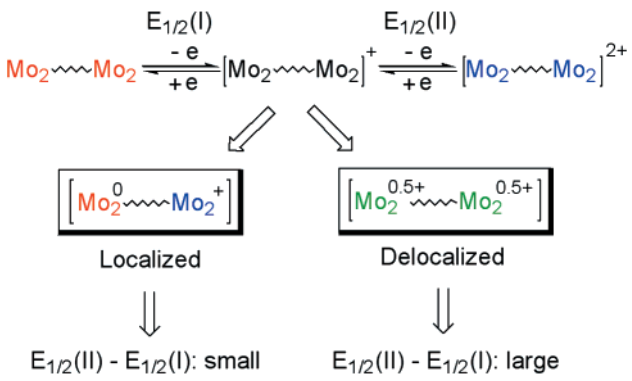

tion occurs. In the case of the oxalate linker, full delocalization seems likely, while in the other two cases what occurs may be best described as polarization of the π electron density in the bridges.

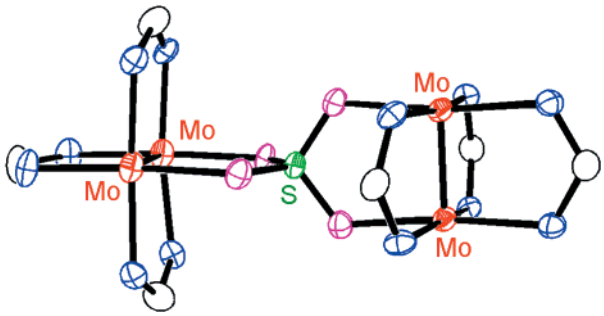

FIGURE 6. Molecular core structure of pair **13** showing two essentially perpendicular Mo_2 units joined by a SO_4^{2-} anion.

Another three compounds containing pairs of Mo_2(DAniF)$_3$ units linked by tetrahedral EO_4^{2-} anions, where E = S, **13**; Mo, **14**; and W, **15**, have also been prepared by a method similar to that mentioned above.[6] They represent the first examples of any kind having this sort of μ_2-η^2,η^2 bridging of two dimetal moieties by any EO_4^{2-} ion. The molecular structures of **13**−**15** are very similar to each other, the structure of **13**, shown in Figure 6, being representative. The EO_4^{2-} linkers hold two Mo_2 units in a perpendicular orientation. All three molecules deviate from the idealized D_{2d} symmetry in the same way, namely, by folding along the lines defined by each pair of two oxygen atoms coordinated to the same Mo_2 unit. The electrochemistry of **13**−**15** is also interesting when compared to that of the 12 pairs described above. Each of the three compounds shows two quasireversible (**13**) or fully reversible (**14**, **15**) features in its CV corresponding to successive oxidation of each of its Mo_2 units. The separations of $E_{1/2}$ values are 228, 311, and 285 mV for **13**−**15**, respectively, which are the largest thus far measured for Mo_2—X—Mo_2 bridged complexes and may be sufficiently large to permit isolation of the singly oxidized species.

Molecular Loops

For dimetal units with only two bridging formamidinate groups in a cisoid relationship, neutral cyclic molecules consisting of two dimetal units, Mo_2^{4+} or Rh_2^{4+}, at the corners have been made by employment of bent dicarboxylate linkers according to the following reaction:

$$2[\textit{cis}\text{-}Mo_2(DAniF)_2(CH_3CN)_4](BF_4)_2 + 2(NBu^n_4)_2(O_2C{-}\square{-}CO_2) \xrightarrow{CH_3CN} [\textit{cis}\text{-}Mo_2(DAniF)_2]_2[O_2C{-}\square{-}CO_2]_2 + 4NBu^n_4BF_4$$

In each case, the yield was essentially quantitative. Five compounds of this type have been structurally characterized,[7] namely, the Mo_2 compounds with malonic acid, **16**; 1,4-phenylenediacetic acid, **17**; homophthalic acid, **18**; and *trans*-cyclopentane-1,2-dicarboxylic acid, **19**, as linkers, and a Rh_2 compound with malonic acid, **20**, as the linker. Structure determinations showed that each M_2 unit retains a paddlewheel conformation consisting of two cis formamidinate paddles and two carboxylate groups. The cores of the molecular structures for **17** and **19** are shown

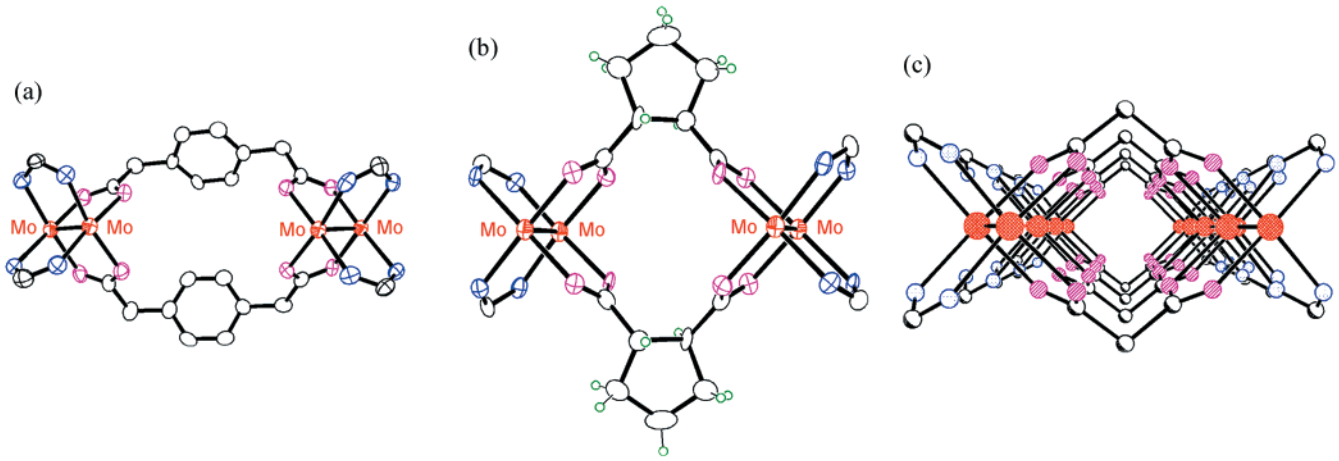

FIGURE 7. (a) Molecular core structure of the phenylendicarboxylate loop **17** with two Mo−Mo coplanar vectors converging at an angle of 103°. (b) Core of the meso pentanedicarboxylate loop **19** with two Mo−Mo vectors essentially parallel. (c) Simplified diagram of the malonate loop **16** showing the channel created by stacking the cores of the molecules in the crystal.

in Figure 7a and b, respectively. Note that **19** is a *meso* isomer having a mirror plane as its only symmetry element. We term assemblies of this type molecular loops.[7]

In the solid state, these compounds, except **17**, show an interesting stacking pattern, giving rise to channel-like cavities by stacking molecular loops directly in register. This is illustrated for **16** in Figure 7c. The solution structures of these compounds have been investigated by ^{1}H NMR spectroscopy. For **16**, **17**, and **20**, there is only one type of DAniF ligand, as indicated by the unique methine and methoxy signals. This indicates that all linkers are equivalent in solution. For both **18** and **19**, there is a pair of singlets for methine protons. This indicates that the less symmetrical solid-state structure persists in solution. Evidently these dicarboxylate linkers are less flexible.

Electrochemical studies showed that the separations of the $E_{1/2}$ values for two successive one-electron oxidations are 109, 91, and 179 mV for **16**, **17**, and **18**, respectively. In attempting to understand the variation in the coupling from one compound to another, one might first ask whether it is a simple function of the distance between the Mo_2 units. Qualitatively, such a relationship does exist: the $\Delta E_{1/2}$ values decrease in the order **18** $\gg$ **16** $>$ **17**, and the corresponding distances (Å), 6.272, 6.512, and 9.624, increase in the same order, but there is no quantitative correlation, since the order of distances is **18** $<$ **16** $\ll$ **17**. If we look instead at the number of carbon atoms between the carboxyl groups, there is no correlation since these go in the order 3, 1, and 6, for compounds **18**, **16**, and **17**, respectively. Clearly it is the electronic nature of the connecting groups that controls the extent of communication, but in ways that are not apparent at present. The rich electrochemical behavior in these neutral loops contrasts to that of the ionic compound $\{Mo_4[O_2C(CH_2)_2CO_2]_2(MeCN)_{12}\}(BF_4)_4$, which is not electroactive.[8] For **19**, there is an irreversible electrochemical oxidation, indicating that there is a major change in the structure.

Molecular Triangles

The first neutral molecular triangle derived from quadruply bonded dimolybdenum units was synthesized by reaction of [*cis*-Mo_2(DAniF)$_2$(CH$_3$CN)$_4$](BF$_4$)$_2$ and (Bu$^n_4$N)$_2$(*trans*-1,4-cyclohexanedicarboxylate), a reaction similar to those used to prepare molecular loops. The yellow compound [*cis*-Mo_2(DAniF)$_2$]$_3$[*eq*,*eq*-1,4-$O_2CC_6H_{10}CO_2$]$_3$, **21**, was isolated in essentially quantitative yield and good purity.[9] Its molecular structure is shown in Figure 8a. The midpoints of the Mo_2 bonds define a triangle with the average distance between vertices being 11.16 Å. It is noteworthy that the conformation of the linker, *trans*-1,4-$C_6H_{10}(CO_2)_2$, in **21** is *eq*,*eq*, whereas in **12** the conformation is *ax*,*ax*. The packing of the triangular molecules in **21** is also interesting. As shown in Figure 8b, these are stacked in the crystal, but with alternating orientations differing by about 60° (a $\bar{3}$ axis). Thus, a projection in the stacking direction has a hexagonal cross section, and the channel is filled with disordered CH_2Cl_2 molecules. Compound **21** displays only an irreversible oxidation wave. It was not possible to determine how many electrons were involved, but with essentially no coupling it could be that the +3 species was produced and that the irreversibility is accounted for by the instability of such a highly oxidized species.

There is another neutral molecular triangle with dimetal units derived from paddlewheel complexes, [*cis*-Rh_2(DAniF)$_2$]$_3$[O_2CCO_2]$_3$, **22**,[10] the stacking diagram of which is shown in Figure 9. This compound can be made only by using exactly 1 equiv of the oxalate anion per equivalent of [*cis*-Rh_2(DAniF)$_2$(CH$_3$CN)$_4$](BF$_4$)$_2$. When an excess of the linker is used, a molecular square, [*cis*-Rh_2(DAniF)$_2$]$_4$(O_2CCO_2)$_4$, **23**, is formed (vide infra).[10] It was found that in solution the molecular square **23** is in equilibrium with the molecular triangle **22**. This equilibrium and the electrochemical behavior of the solution will be discussed further in the following section.

Another molecule containing three Mo_2^{4+} units, [Mo_2(DAniF)$_3$]$_3$(1,3,5-$C_6H_3(CO_2)_3$), **24**, has the shape of a mo-

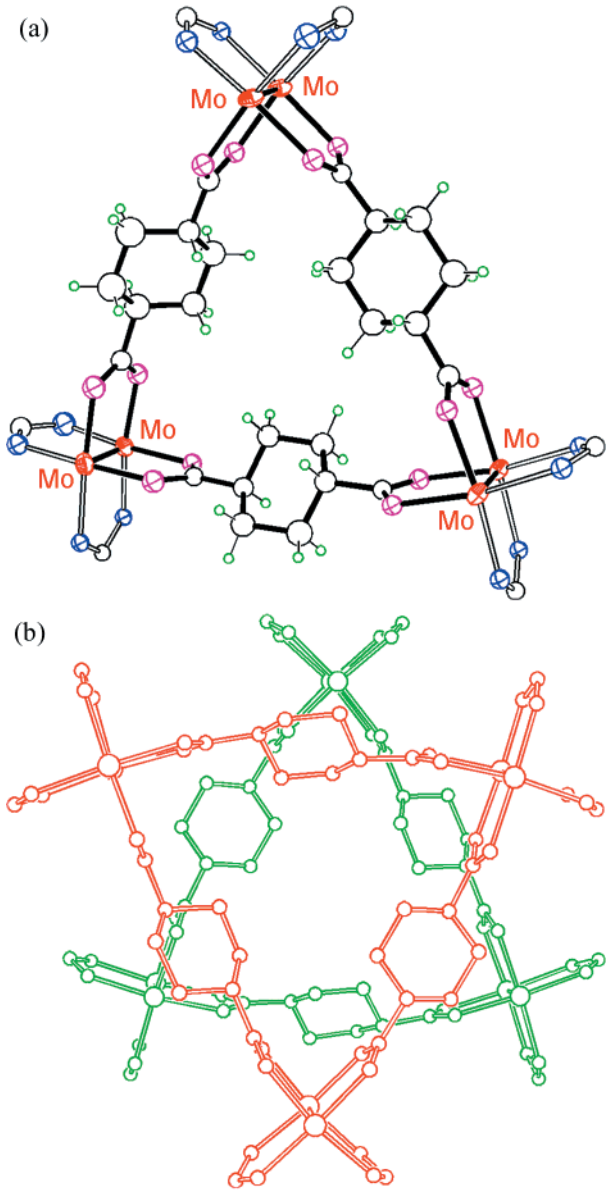

FIGURE 8. (a) The core of the molecular triangle **21** showing three Mo_2 units linked by three cyclohexanedicarboxylate anions. (b) A drawing of the stacking of two molecules of **21**. Notice the rotation of 60° between triangles giving an ABAB··· pattern, which leaves channels in the direction of the stacking.

lecular propeller.[11] It was made by a method similar to one of those used in the preparation of $Mo_2(DAniF)_3$ pairs mentioned above. The orange crystalline compound is soluble in various organic solvents, and it is highly symmetrical in solution, as indicated by its ^1H NMR spectrum. The X-ray structural analysis also showed a highly symmetrical molecule in the solid state. As shown in Figure 10, one $Mo_2(DAniF)_3$ unit is bound to each of the three carboxylate groups of the trimesate anion. The three carboxylate groups are not in the same plane as the aryl group, nor are they perpendicular to it. Thus, the shape of the molecule is that of a propeller, and this molecule is the first molecular propeller of its type. Both the CV and the DPV of **24** show the presence of three one-electron oxidation processes. The total separation is ca.

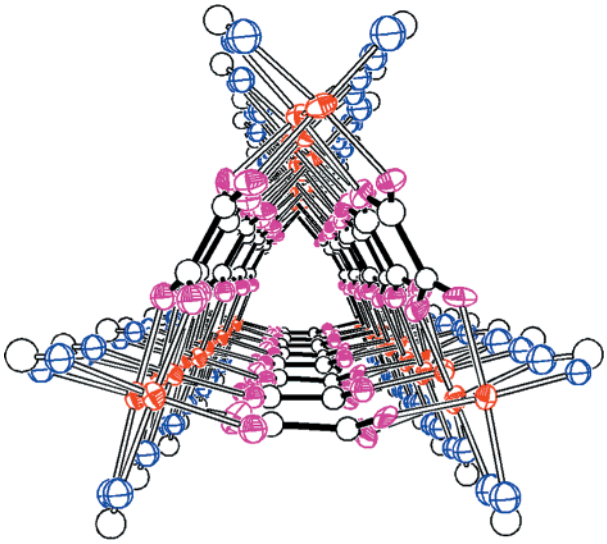

FIGURE 9. A view of the stacking pattern for Rh_2 molecular triangle **22** with oxalate linkers. There are CH_3CN molecules in the central tunnel and axially coordinated to the Rh atoms that have been omitted for clarity. The nonplanarity of the bridging oxalate ions is evident.

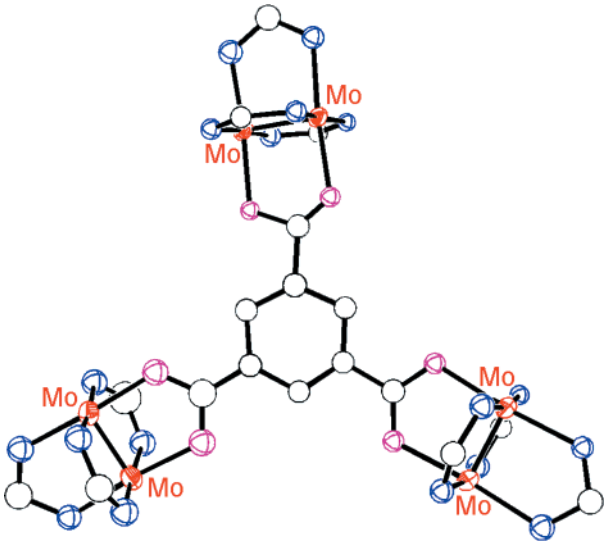

FIGURE 10. A top view of the core of the molecular propeller in **24**.

0.112 V, indicating that there is very little electronic communication between the three Mo_2^{4+} units.

We note here another unique compound also having three Mo_2^{4+} units, but organized around a carbonate ion.[12] Unfortunately, no electrochemistry was reported in this case.

Molecular Squares

Squares are predominant among the supramolecular structures that have been reported containing Pd^{2+} and Pt^{2+} ions. We have also made many of these by employing dimetal units.

Each of the dimetal subunits we have used has been derived from the commonly found paddlewheel structure with negligible torsion angles and each remaining paddle

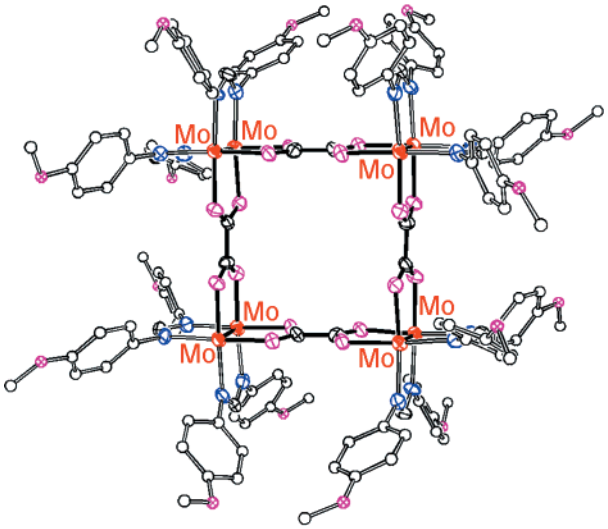

FIGURE 11. Structure of the molecular square **25**, showing four Mo_2 units linked by four oxalate anions.

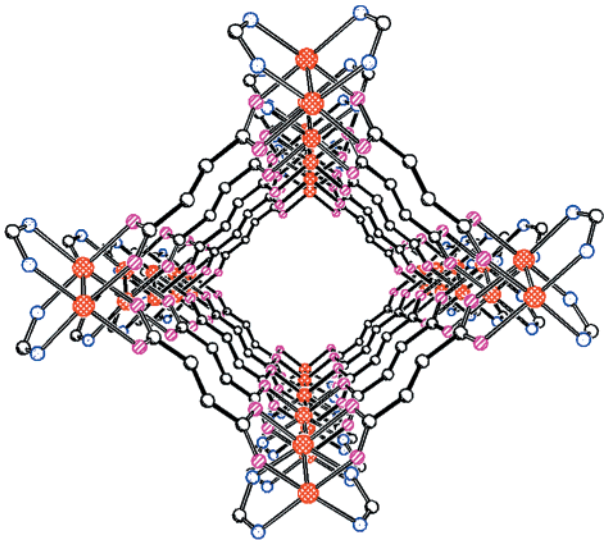

FIGURE 12. Packing of the Mo_2 fumarate square **26** showing the channel created by the stacking of molecules in the crystal.

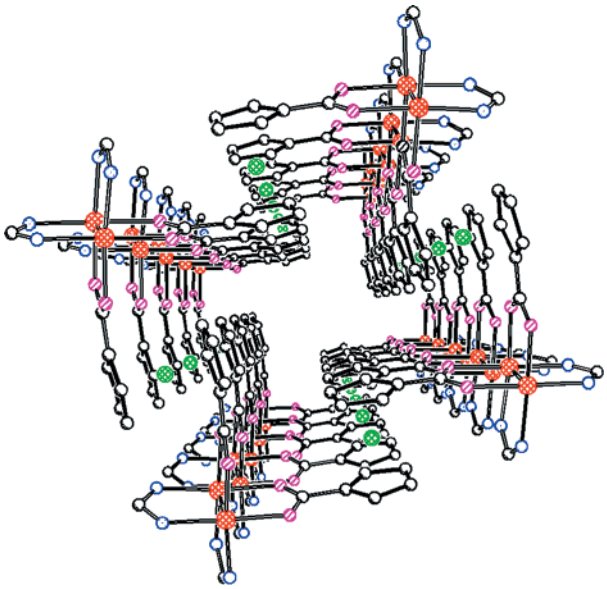

FIGURE 13. Packing of the Mo_2 ferrocene dicarboxylate square **27** showing a complex shaped channel created by the stacking of molecules in the crystal.

forming an angle of about 90° from its neighbors. Not surprisingly, this type of arrangement will most easily give molecular squares following a preparative protocol identical to that described for loops or triangles when rigid linear linkers are employed. The first series of molecular squares was assembled from $Mo_2(DAniF)_2$ subunits.[10,13] As denoted by its carboxylate linker, the squares are oxalate, **25**; fumarate, **26**; ferrocene dicarboxylate, **27**; 4,4′-biphenyldicarboxylate, **28**; acetylenedicarboxylate, **29**; tetrafluoroterephthalate, **30**; and carborane dicarboxylate, **31**. Structural characterization of **25**−**28** revealed a square of dimolybdenum units linked by the dicarboxylate anions. A typical molecular square is shown in Figure 11 for **25**. The area of the square defined by the four Mo_2 corners of each molecule is estimated to be ca. 7 × 7, 9 × 9, 10 × 10, and 15 × 15 Å^2 for **25**−**28**, respectively. The crystal packing is of particular interest. For **25**−**27**, the molecules stack directly on top of each other, resulting in the formation of square channels for **25** and **26** (Figure 12) and one of a more complex shape for **27** (Figure 13). Molecules of **28** are again stacked (Figure 14), but alternate square layers are staggered by ca. 45° so that the squares of every other layer are superposed, giving rise to a channel whose projected cross section has an octagonal shape. Thus, by changing the size and shape of the linker, one can vary not only the size and shape of the oligomers but also of the channels within the crystal. All these four compounds have solvent molecules in intermolecular interstices of the crystal, and also within the square channels. Results of ^{1}H NMR studies on all seven compounds **25**−**31** are consistent with the presence of a highly symmetrical structure in solution.

These compounds also display rich electrochemical behavior which is affected by the nature of the carboxylate linkers. The CV and DPV of **25**, given in Figure 15, show three consecutive one-electron oxidation processes. The differences of 160 mV between the potentials $E_{1/2}$(II) and $E_{1/2}$(I), and 254 mV between $E_{1/2}$(III) and $E_{1/2}$(I), clearly indicate there is electronic rather than mere electrostatic coupling between these processes. The studies for the remaining six compounds revealed also that the total number of electrons involved in oxidations of the dimolybdenum centers is only three, but in these cases the extent of coupling is much lower and may be merely electrostatic.

We have also made similar molecular squares containing Rh_2^{4+} units.[10,14] Since the first one, **23**, was reported, the following six compounds, each noted by the carboxylate linker, have been described: bicyclo[1.1.1]pentane-1,3-dicarboxylate, **32**; tetrafluoroterephthalate, **33**; 1,4-cubanedicarboxylate, **34**; terephthalate, **35**; fumarate, **36**; and *trans*-1,4-cyclohexanedicarboxylate, **37**. In contrast to the preparation of **23** where excess oxalate was required, these six compounds were produced by reactions of a 1:1 ratio of [*cis*-$Rh_2(DAniF)_2(CH_3CN)_4$][BF_4]$_2$ and the corresponding dicarboxylate linkers. The presence of squares

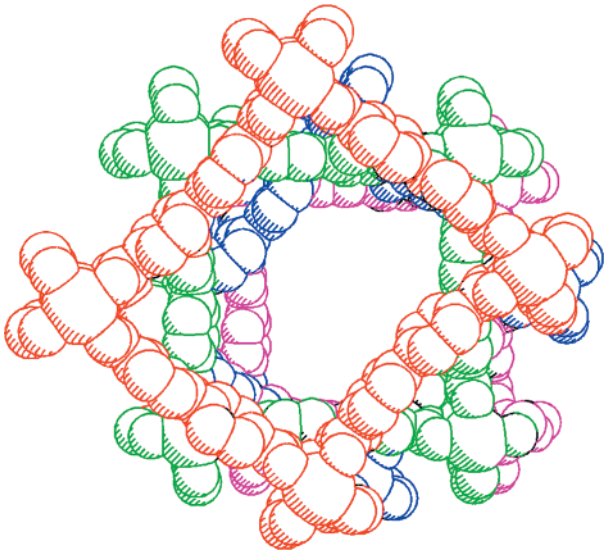

FIGURE 14. Packing of the Mo_2 biphenyldicarboxylate square **28**. Notice the rotation of 45° between consecutive squares in the direction of the stacking; the layers give an ABAB··· pattern.

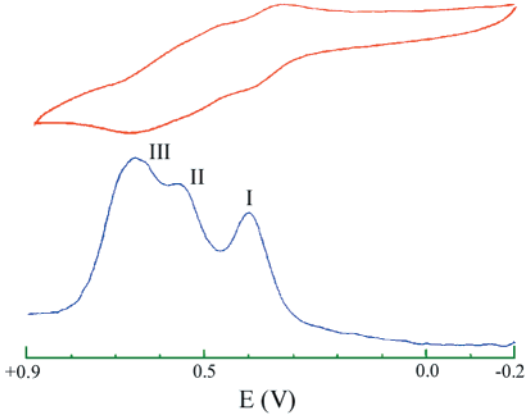

FIGURE 15. Cyclic and differential pulse voltammograms for Mo_2 oxalate square **25**, showing three consecutive one-electron oxidation processes.

has been unequivocally established for every one of the seven compounds by X-ray crystallography. Our slowness in reporting this work (and other things we have done as well) has been due to the fact that the crystallographic determination of such structures is often difficult. However, our practice has been to insist on crystallographic structural data before claiming a compound. Except for the axially coordinated ligands, the structural features of these Rh_2 squares are very similar to those of the Mo_2 ones as shown in Figure 16 for the molecular structure of **34**, and in Figure 17 for the packing diagram of **23**.

As mentioned earlier, there exists an equilibrium in the solution between triangle **22** and square **23**. The ^1H NMR spectra of these two compounds are identical within experimental error. Thus, it is impossible to study the equilibrium by means of the NMR spectra. However, the electrochemical signatures of the square and the triangle are distinctly different. There are three measurable oxidation waves for each complex. For the square **23**, they are at 445, 845, and 1109 mV; those for the triangle **22** are at 509, 1125, and 1441 mV versus the Ag/AgCl couple. Thus,

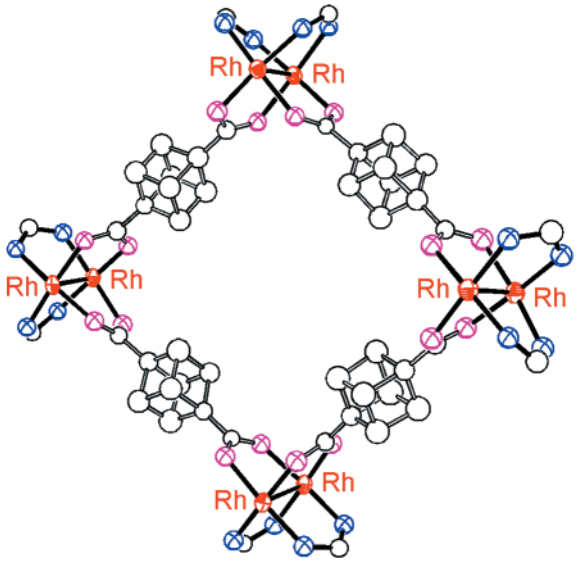

FIGURE 16. Core of the Rh_2 cubanedicarboxylate square **34**.

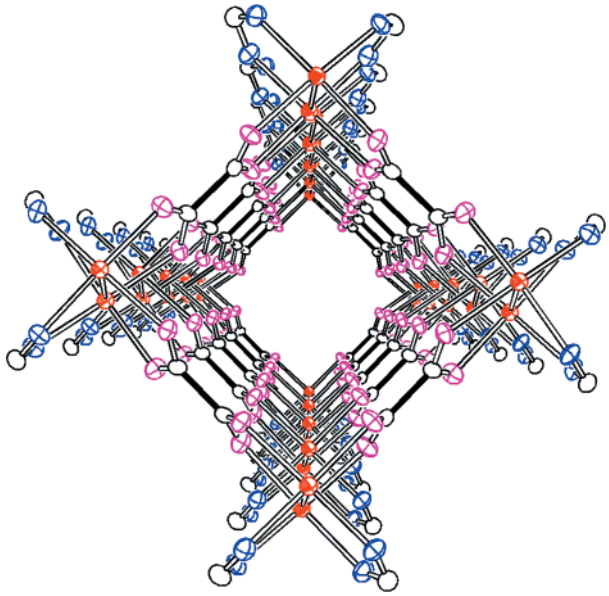

FIGURE 17. A view of the stacking pattern for Rh_2 oxalate square **23**.

by means of electrochemistry, it is possible to study the equilibration of a mixture of squares and triangles, which occurs over a period of several hours. This is the only case known, among systems built from dimetal units, where both triangle and square structures exist for the same linker. With the very flexible cyclohexanedicarboxylate linker, the possibility of finding conditions under which there is a square counterpart of **21** or a triangle counterpart of **37** is far from zero, although we have not yet succeeded in doing so. Perhaps suitable templates are required to direct such crystallization.

Compounds **32**−**37** are also electrochemically active and show two quasireversible waves, each corresponding to 4e oxidations. The first wave is in the range of 240−390 mV, while the second one is in the range of 1040−1170 mV. These electrochemical profiles are stable indefinitely, which is consistent with there being no sort of equilibrium in these solutions.

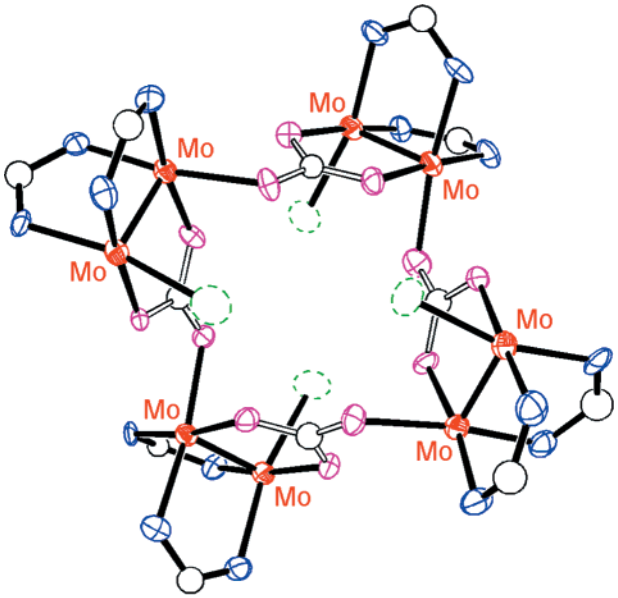

FIGURE 18. Core of the molecular square **38** having S_4 symmetry and four Mo_2 units connected by four CO_3^{2-} anions. The dotted ellipsoids represent water molecules.

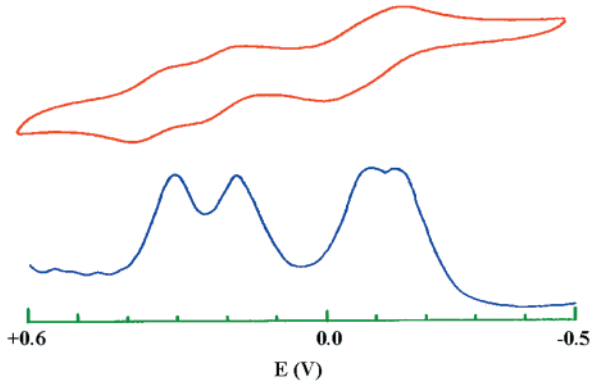

FIGURE 19. Cyclic and differential pulse voltammograms for the Mo_2 carbonate square **38** showing four consecutive one-electron reversible oxidation processes.

Another remarkable molecular square was obtained by the reaction of the usual precursor [*cis*-Mo_2(DAniF)$_2$(CH$_3$CN)$_4$](BF$_4$)$_2$ with (Bu$^n_4$N)$_2$CO$_3$ in wet CH$_3$CN as solvent.[15] The reaction afforded [*cis*-Mo_2(DAniF)$_2$(CO$_3$)(H$_2$O)]$_4$, **38**, the structure of which is shown in Figure 18. The bridging posture of the carbonate ions is at the least a very unusual one; we have not been able to find a prior example in the literature. To complete the set of eight equatorial ligands about each Mo_2^{4+} unit, there is a water molecule on each one. The whole arrangement has approximately S_4 symmetry.

The electrochemistry of this molecule is particularly interesting. Its CV and DPV are shown in Figure 19. The most remarkable feature is that five oxidation states are reversibly available for the first time in any Mo_2 square. These states, corresponding to charges of 0 to +4 on the square, are within a range of about 600 mV. Comparing this result with those of the above Mo_2 squares implies that the electronic communication through the carbonate ion is significantly higher than that possible with dicarboxylate linkers.

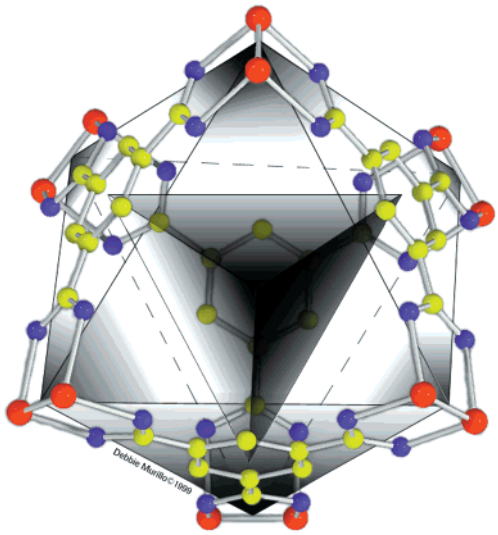

FIGURE 20. The core of the molecular structure of the Mo_2 cage **39**. The drawing emphasizes the pseudo-octahedral distribution of the Mo_2^{4+} units. A cut of the octahedron shows the tetrahedral cavity; the apexes are located at the centers of the rings of the trimesate anions.

Following our work, other groups have also synthesized a few molecular squares, especially with Rh_2^{4+} units.[16]

Molecular Polyhedra

The work described so far has dealt with discrete linear or polygonal arrays. Our next step, logically, was to move from dicarboxylate linkers to tricarboxylate ones. Success in three-dimensional assemblages has been achieved by using the anion of 1,3,5-tricarboxylatobenzene (trimesic acid) as the linker. Molecular cages containing either Mo_2^{4+} (**39**) or Rh_2^{4+} (**40**) units have been assembled by the reaction of 6 equiv of [*cis*-M$_2$(DAniF)$_2$(CH$_3$CN)$_4$](BF$_4$)$_2$ (M = Mo or Rh) with 4 equiv of trimesate anion in CH$_3$CN.[17] The yields are quantitative. The ^{1}H NMR spectra of these two cages indicated a highly symmetrical arrangement: for each cage there was only one resonance for all of the 12 aromatic protons on the four C$_6$H$_3$(CO$_2$)$_3^{3-}$ linkers, and the signals for the 12 DAniF ligands showed them to be equivalent. This highly symmetrical assembly was soon confirmed by X-ray crystallography. The core molecular structure of **39** is shown in Figure 20, while a space-filling diagram of **40** is presented in Figure 21. The centers of the four six-membered rings define a tetrahedron, and the midpoints of the six M_2^{4+} units define an octahedron. The overall idealized symmetry is T_d. However, there is a curious difference between the two structures: there is a disordered "ball" of one CH$_2$Cl$_2$ molecule located inside the Mo_2 cage, while there is a well-ordered CH$_2$Cl$_2$ molecule in the center of the Rh_2 cage.

In electrochemical studies on cage **39**, the CV and DPV showed three distinct reversible oxidation steps at $E_{1/2}$ of 268, 330, and 370 mV versus the Ag/AgCl couple. Based on a calibrated DPV, the ratio of the number of electrons involved in each of these steps is one.

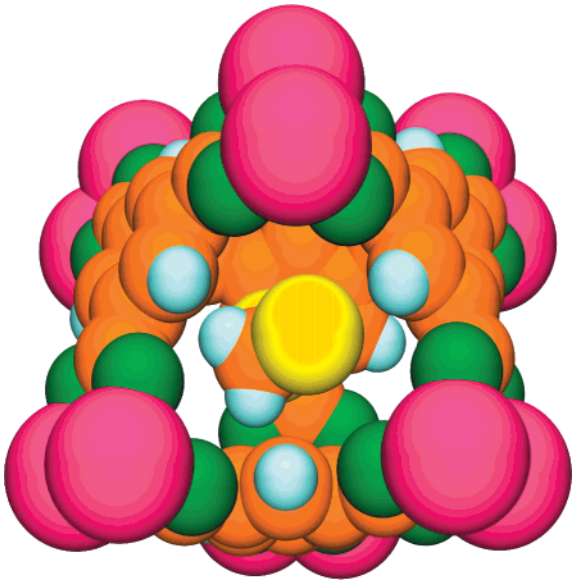

FIGURE 21. A space-filling diagram of the Rh_2 cage **40** showing a CH_2Cl_2 molecule located inside the cage.

Extended Structures

1-D Molecular Tubes. Having demonstrated that moderate-size structures can be made by linking dimetal units, we raised our sights to the goal of making extended arrays of various dimensionalities. To do this, we turned to the idea of employing both equatorial linking and axial linking of M_2 units simultaneously. The use of only axial linking had, of course, already been investigated on many occasions.[18] We intended to take the relatively simple molecular arrays described above and connect them axially to form one-, two-, and three-dimensional polymers. In view of the fact that no Rh_2^{4+} compound lacking axial coordination is known, our next effort was to take advantage of this strong preference for axial coordination in Rh_2 systems. We used compounds **20** and **23** as building blocks to achieve more extended supramolecular arrays.

Our first 1-D polymer was made by employing loop **20** and the axial linker *trans*-1,2-bis(4-pyridyl)ethylene (Figure 2). This resulted in the formation of a tubular molecule, $\{[Rh_2(DAniF)_2]_2(O_2CCH_2CO_2)_2(NC_5H_4CHCHC_5H_4N)_2\}_n$, **41**.[19] A view of its extended structure as well as a schematic representation, showing how the loops are related alternately by centers of inversion and two-fold axes, is shown in Figure 22. Interestingly, there are no guest solvent molecules inside the tubes. Reaction of **20** with the linker octafluoro-4,4′-biphenyldicarbonitrile produced another 1-D molecular tube, $\{[Rh_2(DAniF)_2]_2(O_2CCH_2CO_2)_2(NCC_6F_4C_6F_4CN)_2\}_n$, **42**,[20] the extended structure of which is shown in Figure 23a. A mirror plane perpendicular to the plane of the paper bisects the tube. In contrast to **41**, there are CH_2Cl_2 solvent molecules within these tubes.

When the assembly unit was changed from **20** to **23** and the same linker was used, the compound $\{[Rh_2(DAniF)_2]_4(O_2CCO_2)_4(NCC_6F_4C_6F_4CN)_4\}_n$, **43**, was formed, in which there are infinite tubes of square cross section.[19] A portion of the extended structure is shown in Figure 23b, while Figure 23c shows a space-filling drawing of a segment of a tube including one of the entrained CH_2Cl_2 molecules; Figure 23 also gives a schematic representation of this structure.

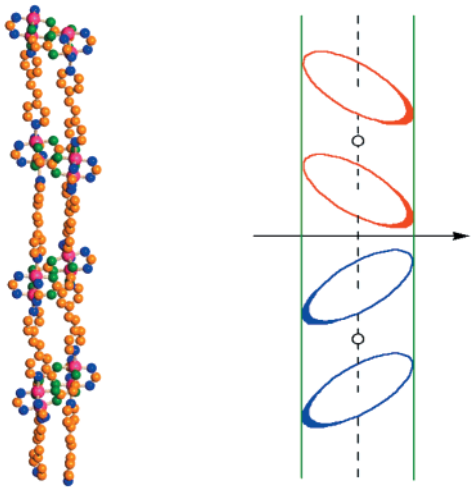

FIGURE 22. On the left, a view of the extended molecular structure of **41**. On the right, a schematic representation showing how the loops are related alternately by centers of inversion and two-fold axes.

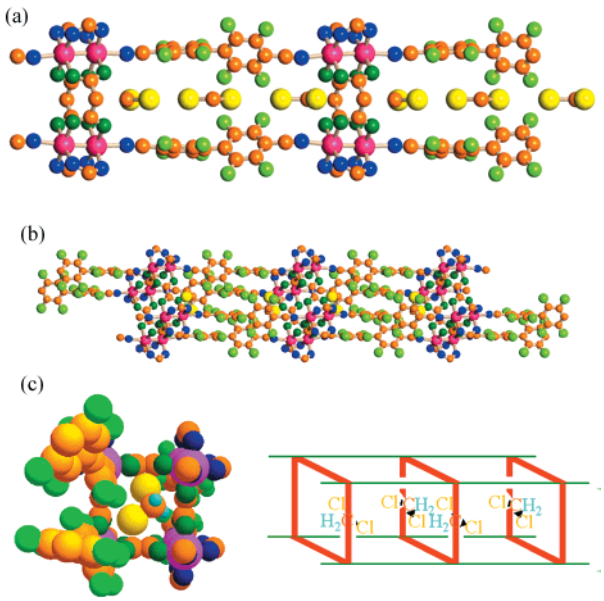

FIGURE 23. (a) A view of the extended structure of **42** showing CH_2Cl_2 molecules located inside the tube. A mirror plane perpendicular to the plane of the paper bisects the tube. (b) A view of the square tube **43** showing CH_2Cl_2 molecules inside the tube. (c) A space-filling drawing of **43** showing a CH_2Cl_2 molecule inside the square cross-sectioned tube. (d) A schematic drawing of the square tube.

Another 1-D extended molecule has been assembled from a three-nitrogen donor linker, tri(4-pyridyl)triazine, but this will be discussed later, because it is, in a sense, a precursor to a three-dimensional structure.

2-D Molecular Tubes. While the formation of the 1-D molecular tubes just described might be considered the "obvious" outcome of linking units of **20** by axial bridges, such a product can be obtained only when the linkers are long enough to keep the bulky *p*-anisyl groups from

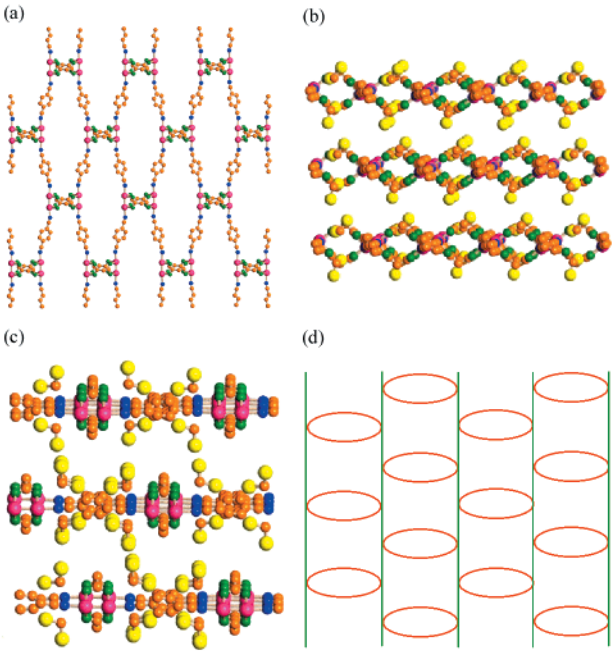

FIGURE 24. (a) A view of the 2-D extended structure of **44**. (b) Intercalating architecture in **44**. (c) Intercalating architecture in **44** viewed from another direction. (d) A schematic drawing of the arrangement of 2-D molecular tubes.

clashing with each other. With a shorter linker, 1,4-dicyanobenzene, major clashes would occur, and therefore a different structure arises for $\{[Rh_2(DAniF)_2]_2(O_2CCH_2CO_2)_2(NCC_6H_4CN)_2\}_n$, **44**.[19] This sheetlike structure is shown in Figure 24a, where CH_2Cl_2 molecules are omitted. In Figure 24b and c, the sheets are viewed from two different edge-on directions, and the CH_2Cl_2 molecules are included; last, the sheets are shown in schematic form in Figure 24d. Each sheet belongs to the two-dimensional space group C*mm*, the highest symmetry possible in a rectangular sheet structure.

3-D Molecular Tubes. Finally, we have reported on the construction of a beautifully elaborate, self-assembled 3-D structure. Earlier results had shown us that the self-assembly process in this system can be stepwise and controllable by varying the stoichiometric ratio of the reactants.

Our approach began with making another 1-D extended molecule. Treatment of the loop **20** with 2 equiv of tri(4-pyridyl)triazine in a $CH_2Cl_2/CHCl_3$ mixture led to the formation of a 1-D, zigzag molecular tunnel, **45**, having the composition $[Rh_2(DAniF)_2]_2(O_2CCH_2CO_2)_2[C_3N_3(C_5H_4N)_3]_2$.[21] A schematic representation of the core is shown in Figure 25a, while its corresponding X-ray structure is shown in Figure 25b. There are several key features in this structure: (1) One loop and two triazine ligands alternate to form a zigzag 1-D tunnel. (2) The planes of two triazine molecules connecting the dirhodium loops are essentially parallel to each other, with an interplanar separation of 3.8 Å, but these two triazine molecules are not superimposed. Instead, within each pair there is a ca. 60° rotation of one relative to the next along a common three-fold axis. (3) Loops are aligned from end to end, and there are no solvent molecules inside the tunnel. (4) Each triazine

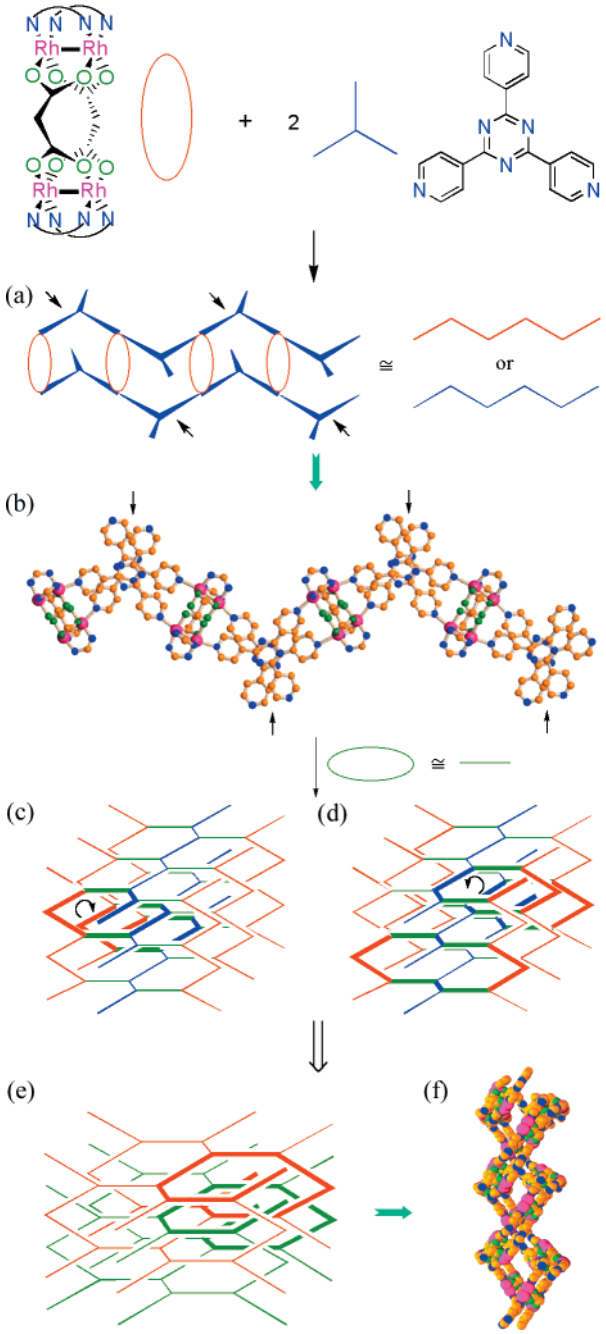

FIGURE 25. (a) A schematic representation of the product of the reaction between loop **20** and tripyridyltriazine. (b) A view of the X-ray structure of **45** showing a zigzag molecular arrangement feature. (c,d) Schematic drawings of the two components present in the 3-D grid **46** formed by addition of one more equivalent of tripyridyltriazine to the 1-D zigzag tunnel **45**. (e) A schematic drawing of the interpenetrating lattice in **46**. (f) A space-filling diagram of the X-ray structure showing the core of the double helix in **46**.

linker uses only two of its three pyridyl nitrogen atoms for coordination. The availability of an unused coordination site on each linker (as indicated by arrows in Figure 25a and b) suggested the possibility of assembling the 1-D tunnels into a 3-D interpenetrating lattice structure, and this, in fact, has been done, as described below.

Reaction of loop **20** with tri(4-pyridyl)triazine in a 3:4 molar ratio, in CH_2Cl_2 solution, gave dark red crystals of

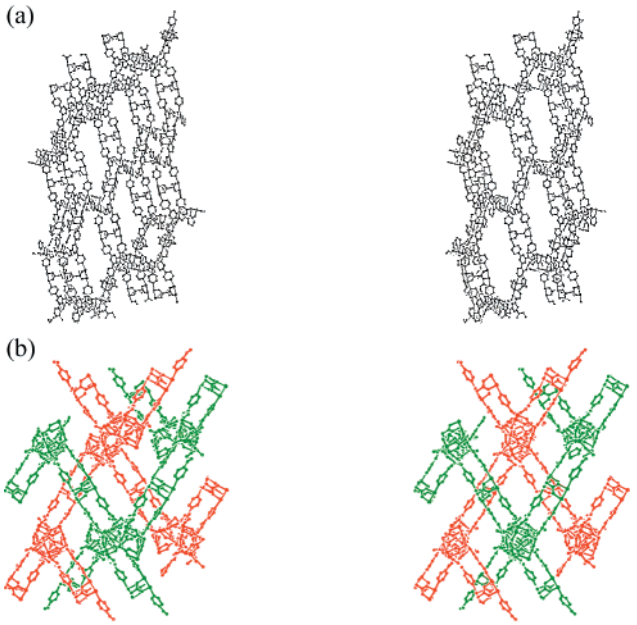

FIGURE 26. Stereoscopic views of (a) one of the helices in **46** emphasizing the spiral hexagon-like stacking and (b) the core of the double helix; for clarity, the right- and left-handed helices are shown in different colors.

$\{[Rh_2(DAniF)_2]_2(O_2CCH_2CO_2)_2\}_3[C_3N_3(C_5H_4N)_3]_4$, **46**.[21] The X-ray structure shows that the additional loop links two zigzag tunnels by using the open nitrogen coordination sites of the triazine ligands. The two essentially parallel triazine planes are staggered, so that the two zigzag tunnels do not lie in the same plane. Two schematic drawings of this grid assembly are shown in Figure 25c and d. When viewed along the *b* axis, there is a spiral hexagon-like stacking, as emphasized by the bold lines. A stereoscopic view is presented in Figure 26a. The left- and right-handed spiral hexagonal units alternate in space and are related by crystallographic inversion centers. Each spiral hexagonal unit has an edge length of ca. 18 Å and is surrounded by six other units. However, all the foregoing description tells only half the story. The two networks shown in Figure 25c and d are both present in the same crystal and interpenetrate each other in such a way that they are related by two-fold axes. The interpenetration of these two networks is shown schematically in Figure 25e, and a stereoscopic view is shown in Figure 26b. Therefore, when viewed along the *b* axis, a single spiral hexagonal unit becomes a double helix, as shown by a space-filling diagram, Figure 25f. The pitch of the helix is ca. 45 Å, and the width is ca. 27 Å. Each such helix is surrounded by six other helices.

Outlook

It is satisfying that in less than three years, so many interesting supramolecular structures have already been made by using metal−metal bonded units as building blocks. What does the future hold? The short answer is, abundant opportunities for further development. To be more specific, there are at least three directions for the work to go. One is the elaboration of still other, more complex structures. Because the lengths and geometries of both the equatorial and the axial linkers can be controlled independently, the possibilities for more diverse two- and three-dimensional structures are vast.

A second opportunity for further development is afforded by the large number of M_2^{n+} units whose utility in this kind of chemistry is still to be explored. Only recently have the first compounds been made with dirhenium units.[22] There are also many as-yet untested ways to design the blocking ligands that are used to limit and direct the steric preferences of the dimetal units. The many different M_2^{n+} units have different spectroscopic, magnetic, and electrochemical properties, and therefore so will the arrays to which they belong.

The third direction that further development may take is to explore the properties of the various supramolecular arrays as designed hosts for small to medium size guest molecules. As the results outlined above clearly indicate, it is possible to vary the size of holes, interstices, and channels angstrom by angstrom. Thus, for example, systems could be designed to selectively remove one noble gas from a mixture containing both larger and smaller ones. Perhaps more interesting is the use of the redox properties of the squares to turn off and on their affinity for anions; in an oxidized (cationic) state, they would readily entrap suitably sized anions and then, when reduced to a neutral condition, disgorge them.

Financial support was provided by the National Science Foundation. Some of the results cited here were obtained by Dr. J. P. Donahue, who is supported by an NIH postdoctoral fellowship. Valuable contributions to the crystallography were made by Dr. L. M. Daniels. Finally, we thank the Texas A&M University for continuing support of the Laboratory for Molecular Structure and Bonding, and Johnson Matthey for a generous loan of $RhCl_3$.

References

(1) See, for example: (a) Fujita, M. Metal-Directed Self-Assembly of Two- and Three-Dimensional Synthetic Receptors. *Chem. Soc. Rev.* **1998**, *27*, 417−426 and references therein. (b) Leininger, S.; Olenyuk, B.; Stang, P. J. Self-Assembly of Discrete Cyclic Nanostructures Mediated by Transition Metals. *Chem. Rev.* **2000**, *100*, 853−908 and references therein. (c) Holliday, B. J.; Mirkin, C. A. Strategies for the Construction of Supramolecular Compounds through Coordination Chemistry *Angew. Chem., Int. Ed.* **2001**, *40*, 2022−2043 and references therein.

(2) Cotton, F. A.; Walton, R. A. *Multiple Bonds Between Metal Atoms*, 2nd ed.; Clarendon Press: Oxford, U.K., 1993.

(3) Chisholm, M. H.; Cotton, F. A.; Daniels, L. M.; Folting, K.; Huffman, J.; Iyer, S.; Lin, C.; Macintosh, A. M.; Murillo, C. A. Compounds in Which the Mo_2^{4+} Unit Is Embraced by Two or Three Formamidinate Ligands Together with Acetonitrile Ligands. *J. Chem. Soc., Dalton Trans.* **1999**, 1387−1391.

(4) Cotton, F. A.; Lin, C.; Murillo, C. A. Coupling Mo_2^{n+} Units Via Dicarboxylate Bridges. *J. Chem. Soc., Dalton Trans.* **1998**, 3151−3153.

(5) Cotton, F. A.; Donahue, J. P.; Lin, C.; Murillo, C. A. The Simplest Supramolecular Complexes Containing Pairs of Mo_2(formamidinate)$_3$ Units Linked with Various Dicarboxylates: Preparative Methods, Structures, and Electrochemistry. *Inorg. Chem.* **2001**, *40*, 1234−1244.

(6) Cotton, F. A.; Donahue, J. P.; Murillo, C. A. Quadridentate Bridging EO_4^{2-} (E = S, Mo, W) Ligands and Their Role as Electronic Bridges. *Inorg. Chem.* **2001**, *40*, 2229−2233.

(7) Cotton, F. A.; Lin, C.; Murillo, C. A. Connecting Pairs of Dimetal Units To Form Molecular Loops. *Inorg. Chem.* **2001**, *40*, 472−477.

(8) This is also the only example of a molecular loop containing Mo_2^{4+} units that preceded those we have made: Whelan, E.; Deveraux, M.; McCann, M.; McKee, V. Non-Polymeric Molybdenum(II) Complexes of Dicarboxylic Acids: Synthesis, Structure and Catalytic Properties. *Chem. Commun.* **1997**, 427−428.
(9) Cotton, F. A.; Lin, C.; Murillo, C. A. A Neutral Triangular Supramolecule Formed by Mo_2^{4+} Units. *Inorg. Chem.* **2001**, *40*, 575−577.
(10) Cotton, F. A.; Daniels, L. M.; Lin, C.; Murillo, C. A. Square and Triangular Arrays Based on Mo_2^{4+} and Rh_2^{4+} Units. *J. Am. Chem. Soc.* **1999**, *121*, 4538−4539.
(11) Cotton, F. A.; Lin, C.; Murillo, C. A. A Molecular Propeller with Three Quadruply-bonded Blades. *Inorg. Chem. Commun.* **2001**, *4*, 130−133.
(12) Suen, M.-C.; Tseng, G.-W.; Chen, J.-D.; Keng, T.-C.; Wang, J.-C. Novel Cyclic Hexanuclear Complexes Containing Quadruply Bonded Units Joined by μ_6-Carbonate Ions. *Chem. Commun.* **1999**, 1185−1186.
(13) Cotton, F. A.; Lin, C.; Murillo, C. A. Supramolecular Squares with Mo_2^{4+} Corners. *Inorg. Chem.* **2001**, *40*, 478−484.
(14) Cotton, F. A.; Lin, C.; Murillo, C. A.; Yu, S.-Y. Supramolecular Squares with Rh_2^{4+} Corners. *J. Chem. Soc., Dalton Trans.* **2001**, 502−504.
(15) Cotton, F. A.; Lin, C.; Murillo, C. A. Maximum Communication Between Coupled Oxidations of Dimetal Units. *J. Am. Chem. Soc.* **2001**, *123*, 2670−2671.
(16) (a) Bickley, J. F.; Bonar-Law, R. P.; Femoni, C.; MacLean, E. J.; Steiner, A.; Teat, S. J. Dirhodium(II) Carboxylate Complexes as Building Blocks. Synthesis and Structures of Square Boxes with Tilted Walls. *J. Chem. Soc., Dalton Trans.* **2000**, 4025−4027. (b) Bonar-Law, R. P.; McGrath, T. D.; Bickley, J. F.; Femoni, C.; Steiner, A. Dirhodium(II) Carboxylate Complexes as Building Blocks. Synthesis of Dimeric Species as Connectors for Macrocycles. *Inorg. Chem. Commun.* **2001**, *4*, 16−18. (c) Schiavo, S. L.; Pocsfalvi, G.; Serroni, S.; Cardiano, P.; Piraino, P. Self-Assembly of Square Molecular Boxes Containing Dirhodium(II,II) Units. *Eur. J. Inorg. Chem.* **2000**, 1371−1375.
(17) (a) Cotton, F. A.; Daniels, L. M.; Lin, C.; Murillo, C. A. The Designed 'Self-assembly' of A Three-dimensional Molecule Containing Six Quadruply-bonded Mo_2^{4+} Units. *Chem. Commun.* **1999**, 841−842. (b) Cotton, F. A.; Lin, C.; Murillo, C. A. Neutral Dodecanuclear Supramolecular Complexes Containing Dimetal Units Linked by the Trimesate Anion. *Inorg. Chem.* **2001**, *40*, in press.
(18) See, for example: (a) Cotton, F. A.; Dikarev, E. V.; Petrukhina, M. A.; Stiriba, S.-E. Studies of Dirhodium Tetra(trifluoroacetate). 5. Remarkable Examples of the Ambidentate Character of Dimethylsulfoxide. *Inorg. Chem.* **2000**, *39*, 1748−1754. (b) Cotton, F. A.; Dikarev, E. V.; Petrukhina, M. A.; Stiriba, S.-E. Studies of Dirhodium(II) Tetrakis(trifluoroacetate). 6. The First Structural Characterization of Axial Alkyne Complexes, $Rh_2(O_2CCF_3)_4(Ph_2C_2)_n$ (n = 1, 2). Diphenylacetylene as a Bifunctional Ligand. *Organometallics* **2000**, *19*, 1402−1405.
(19) Cotton, F. A.; Lin, C.; Murillo, C. A. Supramolecular Structures Based on Dimetal Units: Utilization of Both Equatorial and Axial Connections. *Chem. Commun.* **2001**, 11−12.
(20) Cotton, F. A.; Lin, C.; Murillo, C. A. Controlling the Dimensionality of Metal−Metal Bonded Rh_2^{4+} Polymers by the Length of the Linker. *Inorg. Chem.* **2001**, *40*, in press.
(21) Cotton, F. A.; Lin, C.; Murillo, C. A. The First Dirhodium-based Supramolecular Assemblies with Interlocking Lattices and Double Helices. *J. Chem. Soc., Dalton Trans.* **2001**, 499−501.
(22) (a) Nelson, K. J.; McGaff, R. W.; Powell, D. R. A Tetranuclear Dianion Consisting of Linked Dirhenate Units Arranged in An Infinite One-Dimensional Chain Through Ligand-Ligand Hydrogen Bonding in the Solid State. *Inorg. Chim. Acta* **2000**, *304*, 130−133. (b) Bera, J. K.; Angaridis, P.; Cotton, F. A.; Petrukhina, M. A.; Fanwick, P. E.; Walton, R. A. Incorporating Multiply Bonded Dirhenium Species $[Re_2]^{n+}$ (n = 4 or 5) into Assemblies Containing Two or More Such Units. *J. Am. Chem. Soc.* **2001**, *123*, 1515−1516.

AR010062+